Quantitative Analysis of PlanktoScope Data: a powerful tool for exploring ecosystem function

Dr. Darren Whitehead

darren.a.whitehead@gmail.com

Shark Research Mexico

Dr. Damien Olivier

Universidad Autónoma de Baja California Sur

Dr. Rogelio González-Armas

Centro Interdisciplinario de Ciencias Marinas del Instituto Politécnico Nacional

Dr. Christine Band-Schmidt

Centro Interdisciplinario de Ciencias Marinas del Instituto Politécnico Nacional

Dr. Ismael Gárate-Lizárraga

Centro Interdisciplinario de Ciencias Marinas del Instituto Politécnico Nacional

Jay Gutiérrez

New Atlantis Labs

Research Article

Keywords: automated sampling, planktoscope, planktonic communities, machine learning

Posted Date: July 1st, 2026

DOI: https://doi.org/10.21203/rs.3.rs-9987361/v1

Additional Declarations: No competing interests reported.

Abstract

Plankton communities are essential to aquatic ecosystems, driving primary production (phytoplankton) and global biogeochemical cycles. However, traditional methods for identifying and monitoring plankton are time- and labor-consuming and require a high level of expertise, which may limit large spatio-temporal studies. This study evaluated the effectiveness of the PlanktoScope, an open-source, automated imaging system for monitoring changes in plankton community composition in the coastal waters of La Paz Bay, Mexico. Over a 3-month period from September to November 2024, weekly plankton samples were collected, and the planktonic organisms were identified and counted using the automated classification of the PlanktoScope coupled with the web-interfaced Ecotaxa. A total of 28 taxa were identified, most of them at the genus level, with *Chaetoceros* (Bacillariophyta) dominating the planktonic assemblages. The PlanktoScope successfully highlighted a local temporal shift in planktonic composition during the studied period, between the warm season (September–October) and the warm–cold season transition (November). This shift was mainly driven by a collapse in planktonic cell abundance and an increase in Copepoda and Cyanobacteria biomass. The detected collapse of the autotroph Bacillariophyta (mainly diatoms) corresponded with a decrease in Chlorophyll-a concentrations detected from satellite images. Although the size spectrum revealed a planktonic assemblage dominated by small-size organisms, variation in the biomass distribution among size bins varied throughout the studied period. Our findings highlight the PlanktoScope's potential for high-frequency, cost-effective plankton monitoring. However, while promising, further validation over larger spatio-temporal scales covering different oceanographic contexts is necessary.

Introduction

Plankton are fundamental components of aquatic ecosystems, playing critical roles in food webs and climate regulation. These microscopic organisms, including phytoplankton and zooplankton, support a wide range of marine and freshwater species and contribute to global biogeochemical cycles (Calbet and Landry 2004; Field et al. 1998; Mitra et al. 2014; Steinberg and Landry 2017). Furthermore, plankton dynamics, by rapidly responding to environmental changes, are indicators of ocean health and provide critical insights for predicting the impacts of climate change, ocean acidification, and other anthropogenic stressors (Ajani et al. 2018; Henson et al. 2018, 2021; Ratnarajah et al. 2023).

Traditional plankton sample analyses, based on microscopy, benefit from a high resolution in organism identification by experts but are labor and time-intensive, making large-scale studies difficult to achieve (Álvarez et al. 2014; First and Drake 2012). Therefore, there is a need to perform high-frequency plankton monitoring, with efficient and automated methods available to a larger panel of researchers. Recent advancements in automated plankton processing techniques, with the help of machine learning, have significantly improved the efficiency and accuracy of sample analysis and taxonomic identification (Lombard et al. 2019; Ohman et al. 2019; Orenstein et al. 2022). These innovations are revolutionizing plankton ecology by facilitating the development of extensive, high-resolution databases that can track

plankton communities and help predict changes at the base of the food web over extended periods of time or spatial scales.

The *PlanktoScope* (https://www.planktoscope.org/) is an innovative open-source tool allowing for high-throughput quantitative imaging which, combined with the web-interfaced Ecotaxa (https://ecotaxa.obs-vlfr.fr), enables to identify and count planktonic organisms, dramatically increasing both the efficiency and scope of monitoring efforts (Pollina et al. 2022). This technological advancement presents a cost-effective option to investigate plankton populations and, thereby, improving our understanding of their roles in biogeochemical cycles, food webs, and climate-related phenomena.

The Bay of La Paz, situated on the southeast coastline of Mexico's Baja California Peninsula, is a rich and diverse marine ecosystem (Urcádiz-Cázares et al. 2021), and has been the subject to numerous plankton research studies (Cervantes-Duarte et al. 2021; Coria-Monter et al. 2024; Muciño-Márquez et al. 2018; Verdugo-Díaz and Gárate-Lizárraga 2018; Villalejo-Fuerte et al. 2005; Whitehead et al. 2020). However, there is a critical need to optimize analytical procedures to minimize the time associated with data processing. In this paper, in a proof-of-concept for exploring ecosystem function framework, we tested the reliability of the planktoscope to provide a quantitative analysis of planktonic assemblage variation during a seasonal transition period in the Bay of La Paz.

Methods

1. Field Sampling

To evaluate short term changes in the plankton community, samples were taken weekly over a 3-month trial period between September and November 2024 at a single station (El Mogote, 24.189 N; 110.375 W) in the coastal waters of the Bay of La Paz (Fig. 1). This period encompasses the transition from the warm to the cold season (November-December) in the region.

Planktonic samples were collected using a phytoplankton net measuring 90 cm in total length, with a 30 cm mouth diameter and a mesh size of 20 µm. At each visit, five-minute horizontal tows were conducted at a depth of approximately 1 meter below the water surface, at a towing speed of approximately 1–2 knots, consistent with standard plankton sampling practices. This pilot sampling effort was designed to provide sufficient samples to evaluate the efficiency and feasibility of the plankton imaging device under field conditions, and to establish a baseline before its implementation in longer-term and larger spatial-scale monitoring of the region. After collection, samples were transferred to glass containers and placed in a cooler, protected from direct sunlight and without ice, at approximately 10°C to maintain organism viability during transport to the laboratory within 2 hours. The volume of water filtered during 5-minute surface tow was approximately equal to 10.92 m^3.

At teach tow, planktonic organisms were collected into a 200 ml PVC cod. The cod contain was then homogenized and a subsample of 3 ml was taken for microscopic analysis using the standard protocol Perruchon et al. (2025) developed for the *PlanktoScope* instrument. Prior to processing, all gathered

samples were filtered using a 300 µm mesh into fresh containers, which could damage fragile taxa, but is a necessary step to remove large organisms that could clog the fluidic systems flow cell within the *PlanktoScope* instrument.

2. Plankton imaging

A total of 200 images were taken for each subsample during the imaging procedure adopting a stop flow method which consists of stopping the pump flow and then acquiring an image, allowing sufficient flow between images ensuring that the same organisms were not repeatably photographed. Raw images collected by the *PlanktoScope* were stored locally on its internal memory and automatically processed using a Python-based library MorphoCut, optimized for large imaging datasets. This library applies a running median (based on five frames) to estimate background, followed by Canny edge detection, dilation, closing, and erosion operations using OpenCV. Regions of interest (ROIs) are extracted from the resulting binary images, and 32 mathematical image descriptors are calculated for each ROI using Scikit-image (Pollina et al. 2022). Metadata entered via the graphical user interface is linked to each ROI. The data, including ROIs and descriptors, are compressed and packaged for exportation.

3. Classification, count, biovolume, and biomass estimations of organisms

Cell images exported from the *PlanktoScope* were classified using the EcoTaxa platform (https://ecotaxa.obs-vlfr.fr) which supports automated and manual annotation classification for the user. Initially, raw images were uploaded to the portal, followed by automatic classification using a pre-trained machine learning model integrated within EcoTaxa. The models were selected based on their relevance to the geographic location and the local taxa; however, their effectiveness is limited by the relatively low number of EcoTaxa users and labeled datasets available for this region. These algorithms assigned preliminary taxonomic labels based on morphological features extracted from the images and then allowed for trained taxonomists the chance to manually review, accept or correct these labels to ensure taxonomic accuracy. Final datasets of accurately identified organisms were exported as raw csv files for statistical analyses. To ensure the clarity and interpretability of the analysis, ambiguous images, such as those with unclear features or overlapping organisms, were excluded from further processing. These instances were primarily attributed to poor image quality such as blurriness, being out of focus, or the presence of potential marine debris that could not be reliably identified.

The counts of organism obtained from the 3 mL subsample were extrapolated to represent the entire 200 mL sample volume, which corresponds to a filtered water volume of 10.92 m^3. For comparative purposes, the data were then extrapolated to a volume of 100 m^3. We also estimated the biovolume of each organism in function of their shape. Planktoscope provides the length (major axis) and the width (minor axis) of each organism. If the length was more than twice higher than the width (elongation > 2), then the organism was considered as an ellipsoid to estimate its biovolume, otherwise it was considered

as a spheroid. This approach provided a simplified but consistent method for quantifying plankton biovolume. The biovolume was then converted to carbon biomass (pgC) using conversion parameters from Menden-Deuer and Lessard (2000).

4. Data Analysis

We kept the maximal taxonomic resolution to the genus level. First, we explored the distribution of the size of the identified organisms, which was considered as the major axis (length) of the cell (µm). Second, we explored the distribution of abundance and carbon biomass of the identified organisms among the different identified groups (mainly genera), merging the 12 samples together. Third, we explored the variability in the plankton composition along the studied period by applying a non-Metrical Multidimensional Distance Scaling (nMDS), with a Bray-Curtis dissimilarity matrix after a square root transformation and a Wisconsin double standardization to decrease the importance of highly dominant groups. We performed the nMDS on both the abundance and carbon biomass at Phylum level to capture the general trend in potential assemblage composition rearrangement. Fourth, we explored the temporal changes of absolute abundance and carbon biomass. Fifth, we determined the size spectrum of the sampled assemblages to characterize how the biomass distribution varies with the body size which can be used as an indicator of food web structure and changes in marine community functioning (Trebilco et al. 2013). We estimated the size (carbon biomass) distribution among size ranges using Normalized Biomass Size Spectrum (NBSS). The NBSS calculation aggregates organisms into logarithmic size bins (0.5 $\log_2$ width), normalizes total carbon biomass by bin width, then fits linear regression to $\log_2$ (normalized biomass) vs. $\log_2$(size). We estimated the NBSS for each sampled month. We used a Bayesian model with Gaussian distribution to fit the regressions. For each month, three Markov chain Monte Carlo (MCMC) with 5,000 iterations were run (burning = 4000; thinning rate = 10). Then, we updated the models with 10,000 iterations (thinning rate = 10), which gave us posterior distributions with 3000 values for each parameter. We used median value of the slope with the 95% credible interval and the proportion of posterior distribution that is lower or higher than zero to assess the relative importance of the relationship.

Ultimately, to support the results obtained by the *PlanktoScope*, we explored the association between planktonic composition changes and variation in the chlorophyll-a (Chl-*a*), a proxy of phytoplankton biomass and primary productivity (Longhurst et al. 1995). Using satellite images, we extracted the Chl-*a* concentrations from September to November 2024 with a spatial resolution of 2.5km and time resolution of 8 days (https://coastwatch.pfeg.noaa.gov/data.html). For each of the 12 weeks, we calculated the mean Chl-*a* concentration at two scales: 1) at the Bay of La Paz scale (latitude: 24.1–25.6 N; longitude: 110.7–110.2 W), to capture the regional variation along the studied period, and 2) in a 5-km wide buffer around the studied site (excluding land area, representing seven cells of 2.5 x 2.5 km) to capture local variation that could be more correlated with the assemblages collected into our samples.

All the analysis were run with the R software (R Development Core Team 2024). The following packages were used: ggplot2 (Wickham 2016), dplyr (Wickham et al. 2023), vegan (Oksanen et al., 2022).

Results

The *PlanktoScope* instrument was successful in obtaining good quality images of organisms in collected samples (Fig. 2) which served as a platform for an initial taxonomic identification. A total of 31,815 objects was photographed, of which 19,259 (60%) cells presented the necessary quality and resolution to be associated with a taxonomic level. We identified 28 different taxonomic groups of plankton, 22 of them were assigned to a genus, 1 to family, 2 to orders, 2 to a Class and 1 kept as a phylum (Table 2).

Table 2
List of identified groups in plankton samples of Bahía de La Paz from September 2024 to November 2024. Trophic group classification is based on Mitra et al. (2023).

Taxa	Taxonomic level	Phylum	Trophic group
Copepoda	Class	Arthropoda	Heterotroph
Bacteriastrum	Genus	Bacillariophyta	Autotroph
Chaetoceros	Genus	Bacillariophyta	Autotroph
Corethron	Genus	Bacillariophyta	Autotroph
Ditylum	Genus	Bacillariophyta	Autotroph
Eucampia	Genus	Bacillariophyta	Autotroph
Guinardia	Genus	Bacillariophyta	Autotroph
Melosira	Genus	Bacillariophyta	Autotroph
Neocalyptrella	Genus	Bacillariophyta	Autotroph
Nitzschia	Genus	Bacillariophyta	Autotroph
Odontella	Genus	Bacillariophyta	Autotroph
Pleurosigma/Gyrosigma	Genus	Bacillariophyta	Autotroph
Proboscia	Genus	Bacillariophyta	Autotroph
Rhizosolenia	Genus	Bacillariophyta	Autotroph
Thalassionema	Genus	Bacillariophyta	Autotroph
Thalassiothrix	Genus	Bacillariophyta	Autotroph
Unidentified diatoms	Phylum	Bacillariophyta	Autotroph
Eutintinnus	Genus	Ciliophora	Heterotroph
Parafavella	Genus	Ciliophora	Heterotroph
Tintinnida	Order	Ciliophora	Heterotroph
Undellidae	Family	Ciliophora	Heterotroph
Trichodesmium	Genus	Cyanobacteria	Autotroph
Dinophysis	Genus	Myzozoa	Mixotroph
Protoperidinium	Genus	Myzozoa	Mixotroph
Pyrocystis	Genus	Myzozoa	Mixotroph
Spatulodinium	Genus	Myzozoa	Mixotroph

Taxa	Taxonomic level	Phylum	Trophic group
Acantharia	Class	Radiozoa	Mixotroph
Spumellaria	Order	Radiozoa	Mixotroph

The size (major axis) of the cells ranged from 91 to 1400 µm, with the Arhropoda and Cyanobacteria containing the largest organisms (Fig. 3, Table 3). The size distribution was relatively narrow with low interquartile values for the Ciliophora and Radioza (Table 3). Most of the Bacillariophyta were of small size (low median value and IQR) but also present some large-size cells (Table 3).

Table 3. Summary of the size (µm) per identified phylum. Minimum size (Min), Maximal size (Max), quartiles (Q1:Q3), interquartile (IQR), and ranges are shown.

	Min	Q1	Q2	Q3	Max	IQR	Range
Arthropoda	104	243	355	578	1167	335	1062
Bacillariophyta	86.8	133	177	250	1269	117	1182
Ciliophora	95	111	119	155	361	44	266
Cyanobacteria	91	275	381	516	1400	241	1309
Myzozoa	91	151	285	358	909	207	818
Radiozoa	91	111	124	178	350	67	260

The abundance of cells was largely dominated by the Bacillariophyta with the diatoms genus *Chaetoceros* as the dominant group. The carbon biomass was also dominated by the Bacillariophyta even if the Arthropoda and Cyanobacteria were also well represented by the class Copepoda and the genus *Trichodesmium*, respectively (Fig. 4A). We observed a switch in the planktonic composition between the period September-October and November (Fig. 4B). In term of relative abundance, while the Bacillariophyta were largely dominant during the period September-October, the Cyanobacteria and, to a less extent, Ciliophora and Arthropoda increased during November (Fig. 4B). Concerning the carbon biomass, the Bacillariophyta generally dominated the assemblage during September and October, but were poorly represented during November, with a domination of Arthropoda and Cyanobacteria during the first and second halves of November, respectively (Fig. 4B). The nMDS supported this planktonic composition change, both in abundance and carbon biomass (Fig. 4C). Stress values of both nMDS (0.039 and 0.082 for abundance and carbon biomass, respectively) indicate good quality of the two-dimensional configuration.

From September to October (weeks 1 to 8), the Bacillariophyta (mainly diatoms) dominated the absolute abundance and carbon biomass (Fig. 5A). A shift occurred in November (week 9 to 12), with a collapse of Bacilliariophyta abundance and biomass, the abundance collapse of diatoms was not numerically offset by other Phylum (Fig. 5A). However, the carbon biomass of Arthropoda drastically increased during the first half of November, and we also observed a notable rise of Cyanobacteria biomass during all November period (Fig. 5B).

The NBSS presented negative slopes during the three monitored months (-0.27 [CI: -0.707–0.16]; -0.355 [CI: -0.746–0.095]; -0.151 [CI: -0.538–0.235]), indicating communities dominated by smaller (and lower trophic level) organisms (Fig. 6A). However, the NBSS varied between the periods September-October and November. While a great majority of the NBSS Bayesian estimated slopes were negative in the former (89.7% and 961% for September and October, respectively), only 77.6% of the slopes were negative in the latter (Fig. 6A), which translates a switch from assemblages largely dominated to less dominated by smaller organisms (Fig. 6B). We also observed changes in the size range Phylum composition along the surveyed period (Fig. 6B). Although the large organisms were almost exclusively represented by Arthropoda during the three surveyed months, the Phylum composition in the other size ranges varied. In October and November, the Bacillariophyta were well-represented in all size ranges except the largest organisms, while during September the small size ranges (small and medium-small) were largely dominated by the Arthropoda and Cyanobacteria.

Finally, the analysis of satellite Chl-*a* concentrations revealed spatial and temporal patterns with notable differences between what occurred at the Bay scale and in the studied site. An increase in Chl-*a* concentration occurred in the Bay of La Paz during November, while the contrary was observed at the El Mogote survey site correlating with the low biomass of Bacillariophyta (Fig. 7).

Discussion

In this preliminary work we aimed to highlight the efficiency of the open-source *PlanktoScope* device to monitor variation in planktonic assemblages in the Bay of La Paz. Although the sample period was short and limited to a proof-of-concept framework, the collected data and *PlanktoScope* cells identification successfully revealed discernible patterns in planktonic composition and distribution throughout the sampling period with a marked shift between the end of the warm season (September-October) and the warm-cold season transition (November).

A total of 28 distinct planktonic taxa were identified, with 22 classified to the genus level and the remainder assigned to higher taxonomic ranks. Taxonomic resolution was therefore relatively limited, because of the low number of EcoTaxa users and labeled datasets available for the region. However, expanding the PlanktonScope's reference imagery to include more robust catalogs of local planktonic species would enhance taxonomic resolution in future studies.

Cells abundance and carbon biomass were dominated by the Bacillariophyta, notably the diatoms genus *Chaetoceros*. Diatom dominance is consistent with prior research within the Bay of La Paz, which has consistently identified diatoms as prominent constituents of the phytoplankton assemblage with higher prevalence during the warm season (Gárate-Lizárraga et al. 2009; Muciño-Márquez et al. 2018; Verdugo-Díaz and Gárate-Lizárraga 2018) while the dinoflagellates (Myzozoa) increased during the cold season, period not monitored in the current study, which may explain the low abundance of this Phylum.

Diatoms were not dominant during all the studied period, as diatoms abundance collapse during November, while the biomass of Arthropoda (Copepoda here) drastically increased in the first half of

November. This planktonic composition shift is supported by the satellite-derived Chl-*a* concentrations. The Chl-*a* concentration increases in the Bay in November, which is the usual observed seasonal pattern in the region (Cervantes-Duarte et al. 2025; López-Martínez et al. 2023) but the local Chl-*a* concentrations dropped at our studied site during November which correlates with the observed decrease in the autotroph Bacillariophyta in our samples.

Under theoretical expectations, NBSS should show negative slopes where nutrient limitations increasingly favor smaller, fast-growing taxa over larger, export-efficient phytoplankton like diatoms (Henson et al. 2021; Litchman et al. 2007; Trebilco et al. 2013). Although the NBSS slopes are negative during the three surveyed months, the transition from Bacillariophyta to Arhtropoda biomass dominance is reflected with lower negative NBSS slopes values in November indicating an increase of larger-size cells. Such spatial or temporal segregation is consistent with earlier observations in La Paz Bay, where seasonal shifts in nutrient availability and water column stratification have been shown to drive community composition changes (Aceves-Medina et al. 2017; Muciño-Márquez et al. 2018). The Phylum composition along the size spectrum seems also to vary along the studied period, which could have implication on ecosystem functioning. However, further longer-term time series are necessary to validate and characterize these dynamics at a higher resolution.

A major challenge in conducting long-term surveys of planktonic communities is the high cost of marine research, often exacerbated by inconsistent funding. The PlanktonScope offers a scalable, efficient, and cost-effective tool for high-frequency monitoring and supporting long-term ecological research by enabling consistent data collection. Its compact design, image-based outputs, and automation features, streamline sample analysis and facilitate rapid assessments of plankton communities. Previous applications in global research and citizen science approaches have validated its ability to document taxonomic and morphological diversity (Pollina et al. 2022), as demonstrated in this pilot study. Notably, the PlanktonScope can detect subtle shifts in community structure, making it a valuable tool for identifying early signs of environmental change. Its affordability lowers the entry barrier for institutions with limited access to advanced laboratory infrastructure.

The present study advances previous research by employing high-frequency, image-based monitoring, enabling enhanced temporal resolution in discerning compositional shifts and providing quantitative morphological data. The integration of morphometric parameters, including height, width, and equivalent diameter, further refines this analysis by yielding size-based metrics that can provide information about ecology, trophic interactions, and sinking rates of organisms (for example in the perspective of calculating carbon flux). Future work should focus on: (1) expanding taxonomic libraries for regional species, (2) incorporating wider size classes to capture the complete size spectra, (3) coupling with environmental data for mechanistic understanding, (4) extending spatio-temporal coverage to resolve transition dynamics. With these improvements, *PlanktoScope* could provide the high-frequency, spatially-distributed observations needed to track ocean ecosystem responses to environmental change.

Declarations

No funding was received to assist with the preparation of this manuscript

Author Contribution

D.W and D.O wrote the main manuscript text and D.O prepared the figures and analysis with the support of D.W. R.G.A, C.B.S and I.M supported the text for the manuscript and added additional technical support for plankton verification. J.G reviewed the final manuscript and provided additional text and comments

Acknowledgement

We thank New Atlantis Labs for supporting this research. We also acknowledge the assistance of colleagues and staff at the Centro Interdisciplinario de Ciencias Marinas del Instituto Politécnico Nacional (CICIMAR-IPN), as well as all those who contributed to field sampling and data analysis.

References

1. Aceves-Medina, G., De Silva-Dávila, R., Cruz-Estudillo, I., Durazo, R., & Avendaño-Ibarra, R. (2017). Influence of the oceanographic dynamic in size distribution of cephalopod paralarvae in the southern Mexican Pacific Ocean (rainy seasons 2007 and 2008). *Latin American Journal of Aquatic Research*, *45*(2), 356–369. https://doi.org/10.3856/vol45-issue2-fulltext-11
2. Ajani, P. A., McGinty, N., Finkel, Z. V., & Irwin, A. J. (2018). Phytoplankton realized Niches Track changing oceanic conditions at a long-term coastal station off Sydney Australia. *Frontiers in Marine Science*, *5*(AUG). https://doi.org/10.3389/fmars.2018.00285
3. Álvarez, E., Moyano, M., López-Urrutia, Á., Nogueira, E., & Scharek, R. (2014). Routine determination of plankton community composition and size structure: A comparison between FlowCAM and light microscopy. *Journal of Plankton Research*, *36*(1), 170–184. https://doi.org/10.1093/plankt/fbt069
4. Calbet, A., & Landry, M. R. (2004). Phytoplankton growth, microzooplankton grazing, and carbon cycling in marine systems. *Limnology and Oceanography*, *49*(1), 51–57. https://doi.org/10.4319/lo.2004.49.1.0051
5. Cervantes-Duarte, R., González-Rodríguez, E., Funes-Rodríguez, R., Ramos-Rodríguez, A., Torres-Hernández, M. Y., & Aguirre-Bahena, F. (2021). Variability of net primary productivity and associated biophysical drivers in bahía de la paz (Mexico). *Remote Sensing*, *13*(9). https://doi.org/10.3390/rs13091644
6. Cervantes-Duarte, R., González-Rodríguez, E., Gómez-Gutierrez, J., David Acevedo-Acosta, J., Valladarez-Alfonso, L., & Ricardo Amaro-Sánchez, L. (2025). Nutrient limitation during anomalously warm periods in the southwestern Gulf of California, Mexico. *Regional Studies in Marine Science*, *90*. https://doi.org/https://doi.org/10.1016/j.rsma.2025.104475.

7. Coria-Monter, E., Monreal-Gómez, M. A., Salas-De-león, D. A., Durán-Campos, E., Rocha-Díaz, F. A., & Torres-Martínez, C. M. (2024, November 1). Processes and mechanisms that determine the planktonic production in the largest bay inside the Gulf of California, Mexico: a synthesis and review. *Latin American Journal of Aquatic Research*. Escuela de Ciencias del Mar. https://doi.org/10.3856/vol52-issue5-fulltext-3206
8. Field, C. B., Behrenfeld, M. J., Randerson, J. T., & Falkowski, P. (1998). Primary production of the biosphere: Integrating terrestrial and oceanic components. *Science*, *281*(5374), 237–240. https://doi.org/10.1126/science.281.5374.237
9. First, M. R., & Drake, L. A. (2012). Performance of the human “counting machine”: Evaluation of manual microscopy for enumerating plankton. *Journal of Plankton Research*, *34*(12), 1025–1041. https://doi.org/10.1093/plankt/fbs068
10. Gárate-Lizárraga, I., Band-Schmidt, C., Aguirre-Bahena, F., & Grayeb-Del Alamo, T. (2009). A multi-species microalgae bloom in Bahía de La Paz, Gulf of California (June 2008). *CICIMAR Oceánides*, *24*(1). https://doi.org/https://doi.org/10.37543/oceanides.v24i1.50
11. Henson, S. A., Cael, B. B., Allen, S. R., & Dutkiewicz, S. (2021). Future phytoplankton diversity in a changing climate. *Nature Communications*, *12*(1). https://doi.org/10.1038/s41467-021-25699-w
12. Henson, S. A., Cole, H. S., Hopkins, J., Martin, A. P., & Yool, A. (2018). Detection of climate change-driven trends in phytoplankton phenology. *Global Change Biology*, *24*(1), e101–e111. https://doi.org/10.1111/gcb.13886
13. Litchman, E., Klausmeier, C. A., Schofield, O. M., & Falkowski, P. G. (2007). The role of functional traits and trade-offs in structuring phytoplankton communities: Scaling from cellular to ecosystem level. *Ecology Letters*, *10*(12), 1170–1181. https://doi.org/10.1111/j.1461-0248.2007.01117.x
14. Lombard, F., Boss, E., Waite, A. M., Uitz, J., Stemmann, L., Sosik, H. M., et al. (2019). Globally consistent quantitative observations of planktonic ecosystems. *Frontiers in Marine Science*. Frontiers Media S.A. https://doi.org/10.3389/fmars.2019.00196
15. Longhurst, A., Sathyendranath, S., Platt, T., & Caverhill, C. (1995). An estimate of global primary production in the ocean from satellite radiometer data. *Journal of Plankton Research*, *17*(6), 1245–1271.
16. López-Martínez, J., Farach-Espinoza, E. B., Herrera-Cervantes, H., & García-Morales, R. (2023). Long-Term Variability in Sea Surface Temperature and Chlorophyll a Concentration in the Gulf of California. *Remote Sensing*, *15*(16). https://doi.org/10.3390/rs15164088
17. Menden-Deuer, S., & Lessard, E. J. (2000). Carbon to volume relationships for dinoflagellates, diatoms, and other protist plankton. *Limnology and Oceanography*, *45*(3), 569–579. https://doi.org/10.4319/lo.2000.45.3.0569
18. Mitra, A., Caron, D. A., Faure, E., Flynn, K. J., Leles, S. G., Hansen, P. J., et al. (2023). The Mixoplankton Database (MDB): Diversity of photo-phago-trophic plankton in form, function, and distribution across the global ocean. *Journal of Eukaryotic Microbiology*, *70*(4). https://doi.org/10.1111/jeu.12972

19. Mitra, A., Castellani, C., Gentleman, W. C., Jónasdóttir, S. H., Flynn, K. J., Bode, A., et al. (2014). Bridging the gap between marine biogeochemical and fisheries sciences; configuring the zooplankton link. *Progress in Oceanography*, *129*(PB), 176–199. https://doi.org/10.1016/j.pocean.2014.04.025
20. Muciño-Márquez, R. E., Gárate-Lizárraga, I., López-Cortés, D. J., Bustillos-Guzmán, J. J., & Hernández-Sandoval, F. E. (2018). Seasonal variation of the phytoplankton community in tuna farms in Bahía de la Paz, southern Gulf of California, Mexico. *Latin American Journal of Aquatic Research*, *46*(5), 1011–1024. https://doi.org/10.3856/vol46-issue5-fulltext-14
21. Ohman, M. D., Davis, R. E., Sherman, J. T., Grindley, K. R., Whitmore, B. M., Nickels, C. F., & Ellen, J. S. (2019). Zooglider: An autonomous vehicle for optical and acoustic sensing of zooplankton. *Limnology and Oceanography: Methods*, *17*(1), 69–86. https://doi.org/10.1002/lom3.10301
22. Oksanen, J., Blanchet, G., Friendly, M., Kindt, R., Legendre, P., McGlinn, D., et al. (2018). vegan: Community Ecology Package. R package version 2.5-2.
23. Orenstein, E. C., Ayata, S. D., Maps, F., Becker, É. C., Benedetti, F., Biard, T., et al. (2022, August 1). Machine learning techniques to characterize functional traits of plankton from image data. *Limnology and Oceanography*. John Wiley and Sons Inc. https://doi.org/10.1002/lno.12101
24. Perruchon, A., Zaccomer, H., & Lombard, F. (2025). *Planktoscope protocol for plankton imaging V.5.*
25. Pollina, T., Larson, A. G., Lombard, F., Li, H., Le Guen, D., Colin, S., et al. (2022). PlanktoScope: Affordable Modular Quantitative Imaging Platform for Citizen Oceanography. *Frontiers in Marine Science*, *9*. https://doi.org/10.3389/fmars.2022.949428
26. R Development Core Team. (2024). R: A language and environment for statistical computing. Vienna, Austria: R Foundation for Statistical Computing. See http://R-project.org/.
27. Ratnarajah, L., Abu-Alhaija, R., Atkinson, A., Batten, S., Bax, N. J., Bernard, K. S., et al. (2023, December 1). Monitoring and modelling marine zooplankton in a changing climate. *Nature Communications*. Nature Research. https://doi.org/10.1038/s41467-023-36241-5
28. Steinberg, D. K., & Landry, M. R. (2017). Zooplankton and the Ocean Carbon Cycle. *Annual Review of Marine Science*, *9*(1), 413–444. https://doi.org/10.1146/annurev-marine-010814-015924
29. Trebilco, R., Baum, J. K., Salomon, A. K., & Dulvy, N. K. (2013, July). Ecosystem ecology: Size-based constraints on the pyramids of life. *Trends in Ecology and Evolution*. https://doi.org/10.1016/j.tree.2013.03.008
30. Urcádiz-Cázares, F. J., Cruz-Escalona, V. H., Peterson, M. S., Marín-Enriquez, E., González-Acosta, A. F., Martínez-Flores, G., et al. (2021). Ecological niche modelling of endemic fish within La Paz Bay: Implications for conservation. *Journal for Nature Conservation*, *60*. https://doi.org/10.1016/j.jnc.2021.125981
31. Verdugo-Díaz, G., & Gárate-Lizárraga, I. (2018). Distribution of functional groups of phytoplankton in the euphotic zone during an annual cycle in Bahía de La Paz, Gulf of California. *CICIMAR Oceánides*, *33*(1). https://doi.org/https://doi.org/10.37543/oceanides.v33i1.227

32. Villalejo-Fuerte, M., Muñetón-Gómez, M. S., Gárate-Lizárraga, I., & García-Domínguez, F. (2005). Gut content, phytoplankton abundance and reproductive season in the black oyster (*Hyotissa hyotis*, LINNÉ, 1758) at Isla Espíritu Santo, Gulf of California. *Journal of Shellfish Research*, *24*(1),
33. Whitehead, D. A., Jakes-Cota, U., Pancaldi, F., Galván-Magaña, F., & González-Armas, R. (2020). The influence of zooplankton communities on the feeding behavior of whale shark in Bahia de La Paz, Gulf of California. *Revista Mexicana de Biodiversidad*, *91*. https://doi.org/10.22201/ib.20078706e.2020.91.3054
34. Wickham, H. (2016). ggplot2: Elegant Graphics for Data Analysis. Springer-Verlag New York, 2016.
35. Wickham, H., François, R., Henry, L., Müller, K., & Vaughan, D. (2023). _dplyr: A Grammar of Data Manipulation_. R package version 1.1.4.

Figures

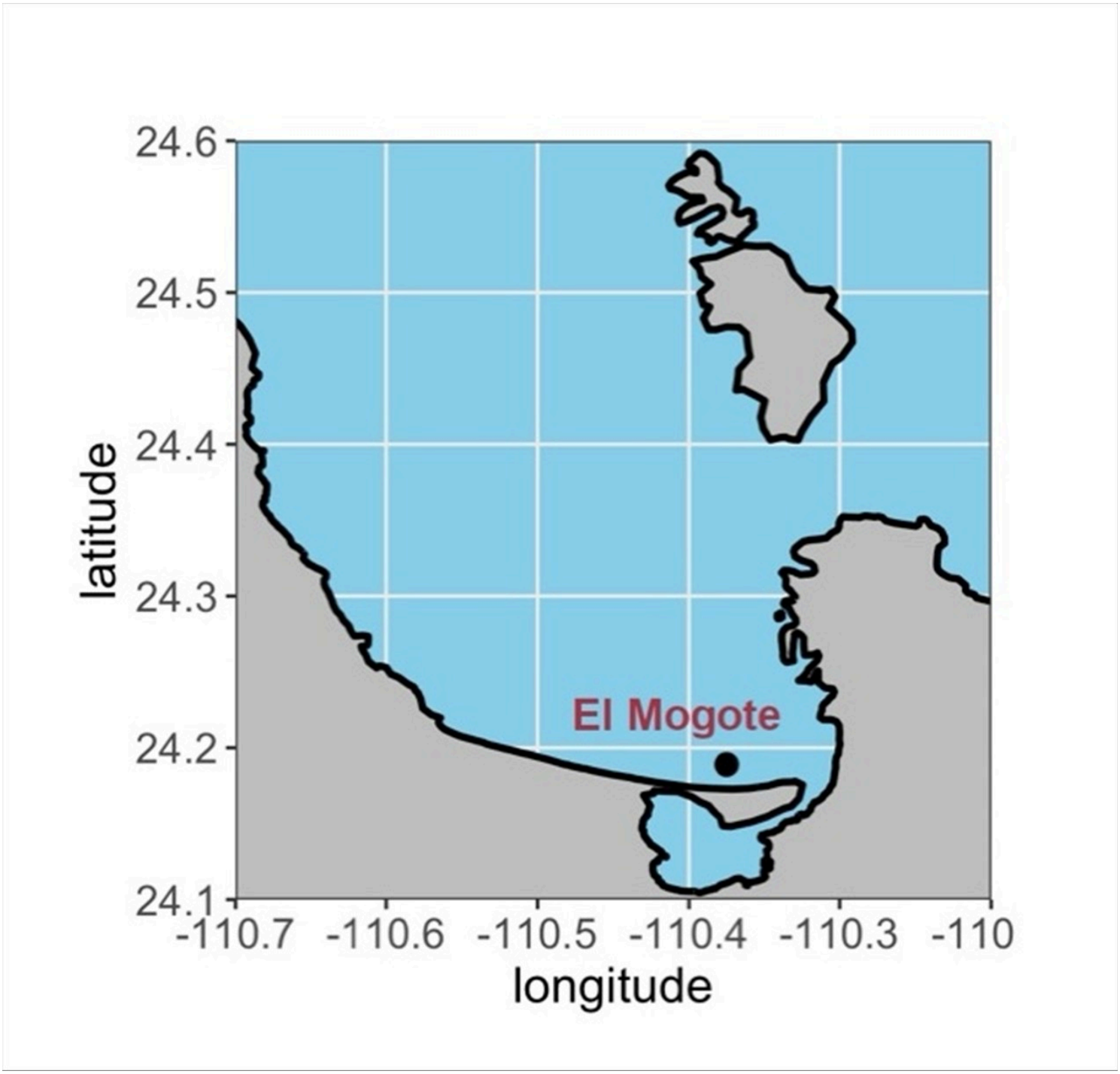

Figure 1

Map of the Bay of La Paz with the location of the sampled station.

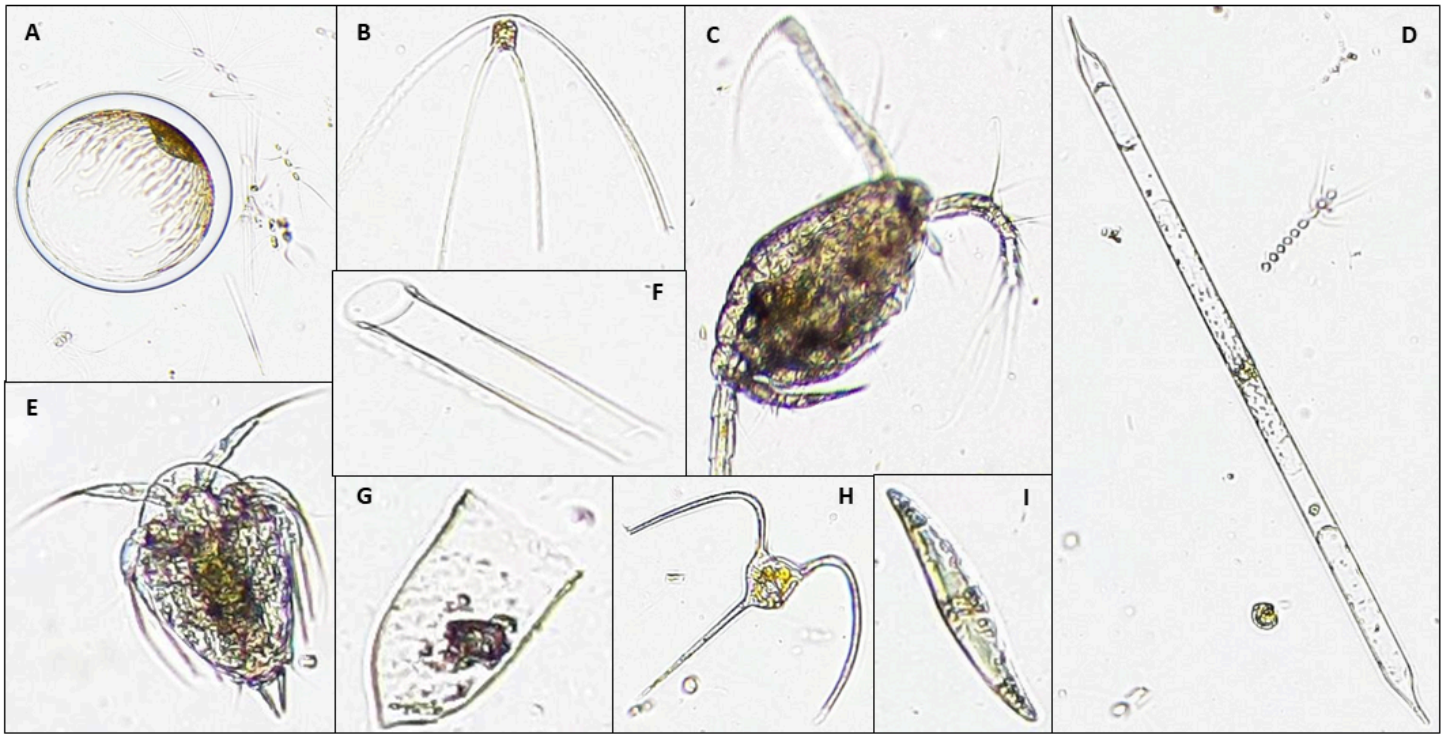

Figure 2

Representative images of phytoplankton and zooplankton organisms captured using the *PlanktoScope* in the Bay of La Paz. (A) *Pyrocystis sp.*, (B) *Chaetoceros sp.*, (C) Copepoda, (D) *Proboscia* sp, (E) Nauplius larva (Crustacea), (F) *Eutintinnus*sp., (G) *Parafavella* sp., (H) *Tripos* sp., (I) *Pleurosigma/Gyrosigma* sp. The images are for an illustrative purpose and the scale may vary between them.

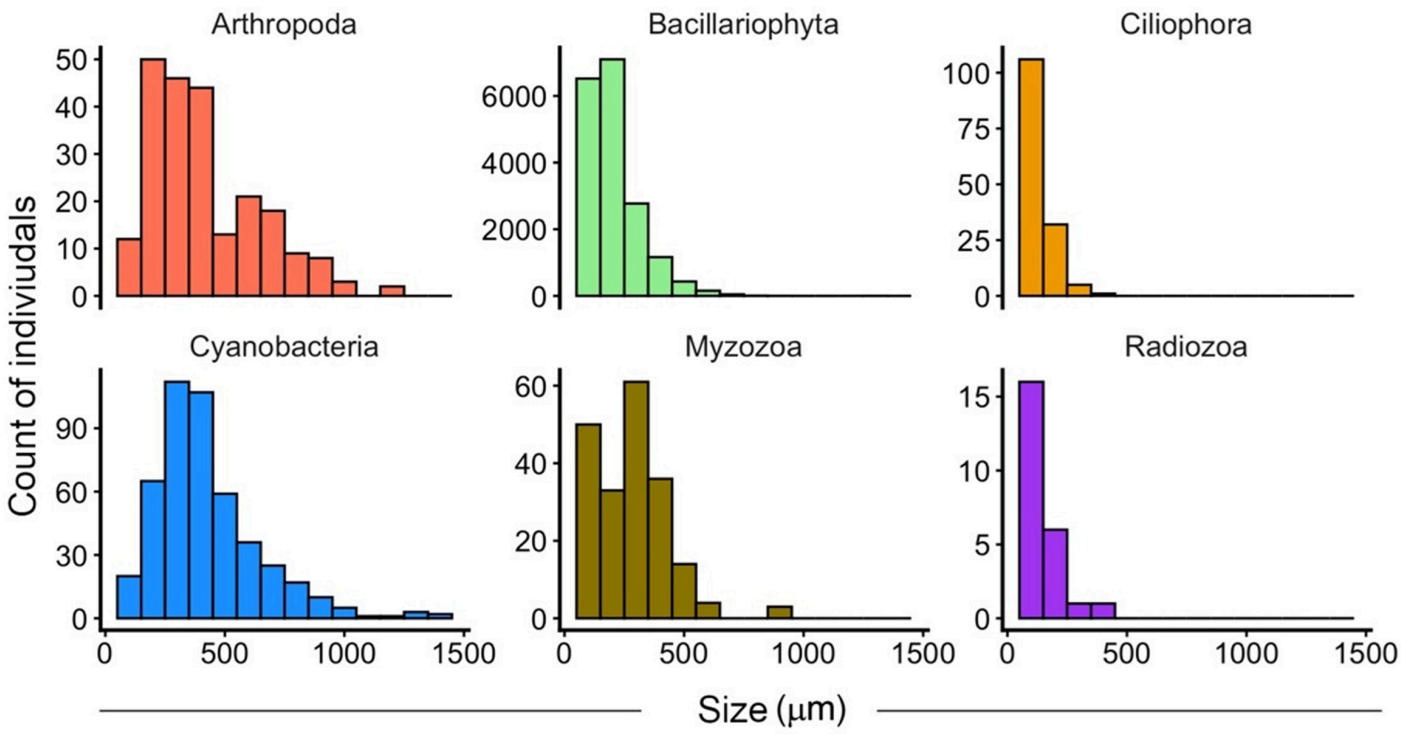

Figure 3

Size characteristics of the identified groups. The size is measured as the major axis (length) of the cell

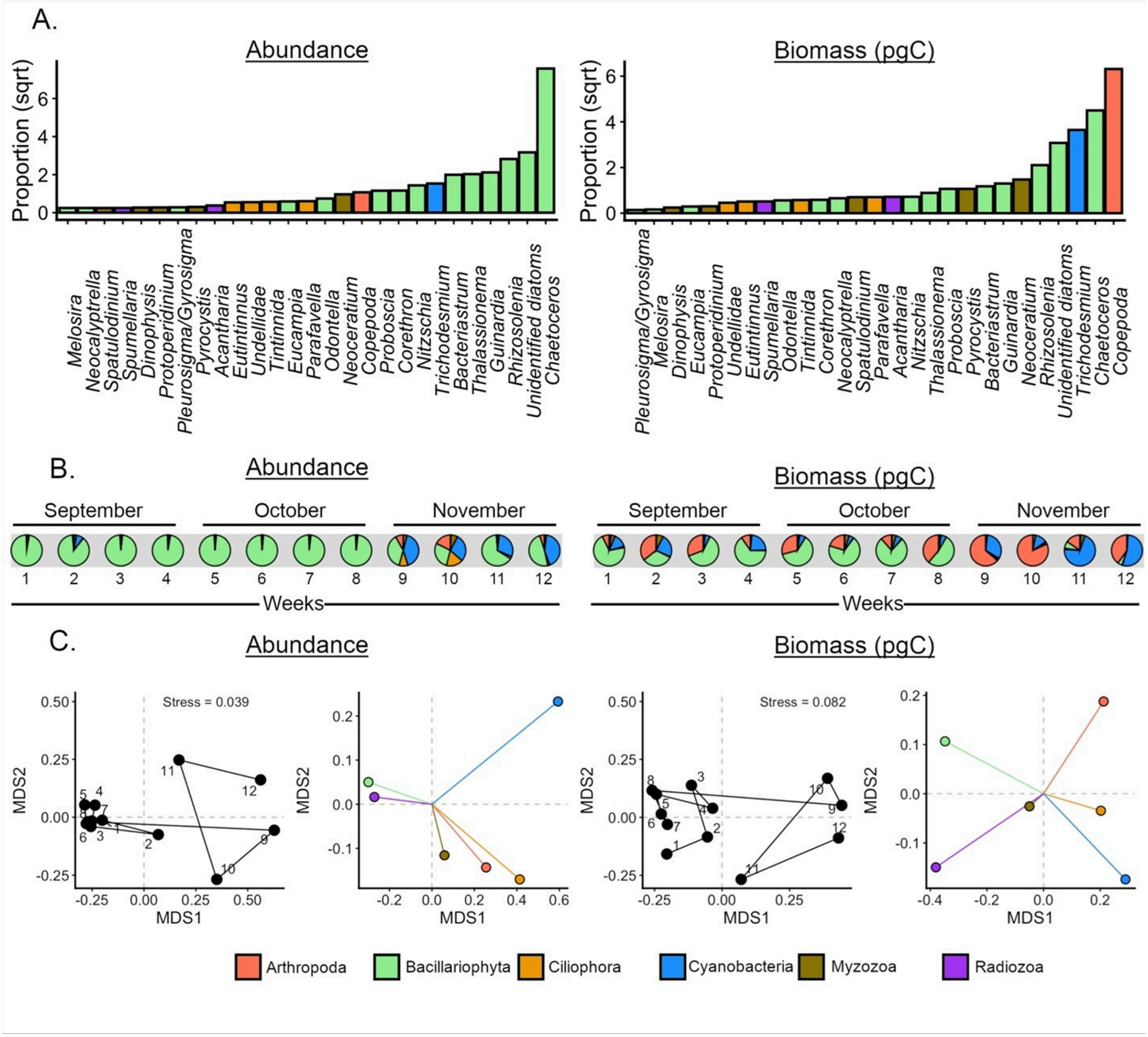

Figure 4

Planktonic composition identified by the *PlanktoScope*. (A) Distribution (in square-root) of relative abundance and biomass (in pgC) among the identified groups. (B) Pieplots illustrating the assemblage composition (abundance and biomass) at the Phylum level along the studied period. (C) nMDS highlighting the variability in planktonic assemblage compositions along the surveyed period. The positions of the 12 weeks (samples) in the two-dimensional space of the nMDS are illustrated and the biplots show the importance of the different Phylum in the observed pattern. In the three panels, Phylum are color-coded.

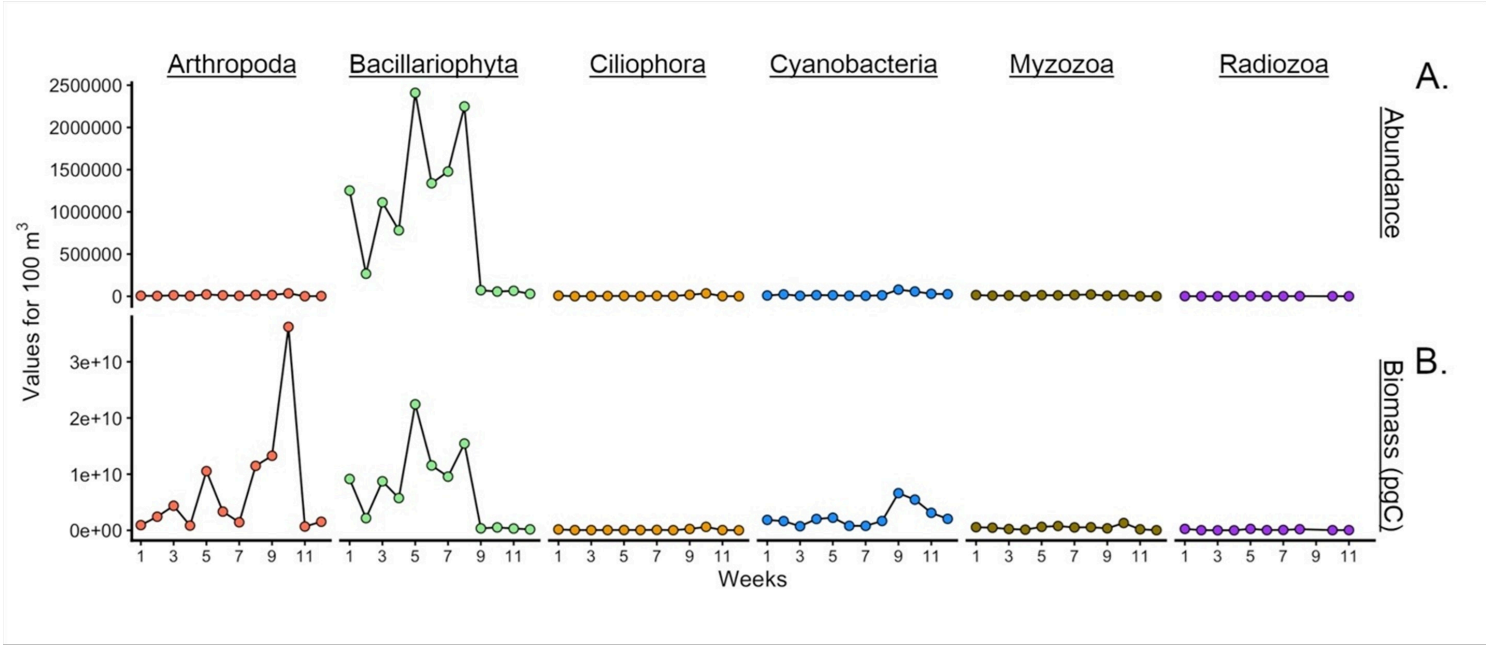

Figure 5

Temporal variation in the planktonic abundance (A) and carbon biomass (B) per Phylum.

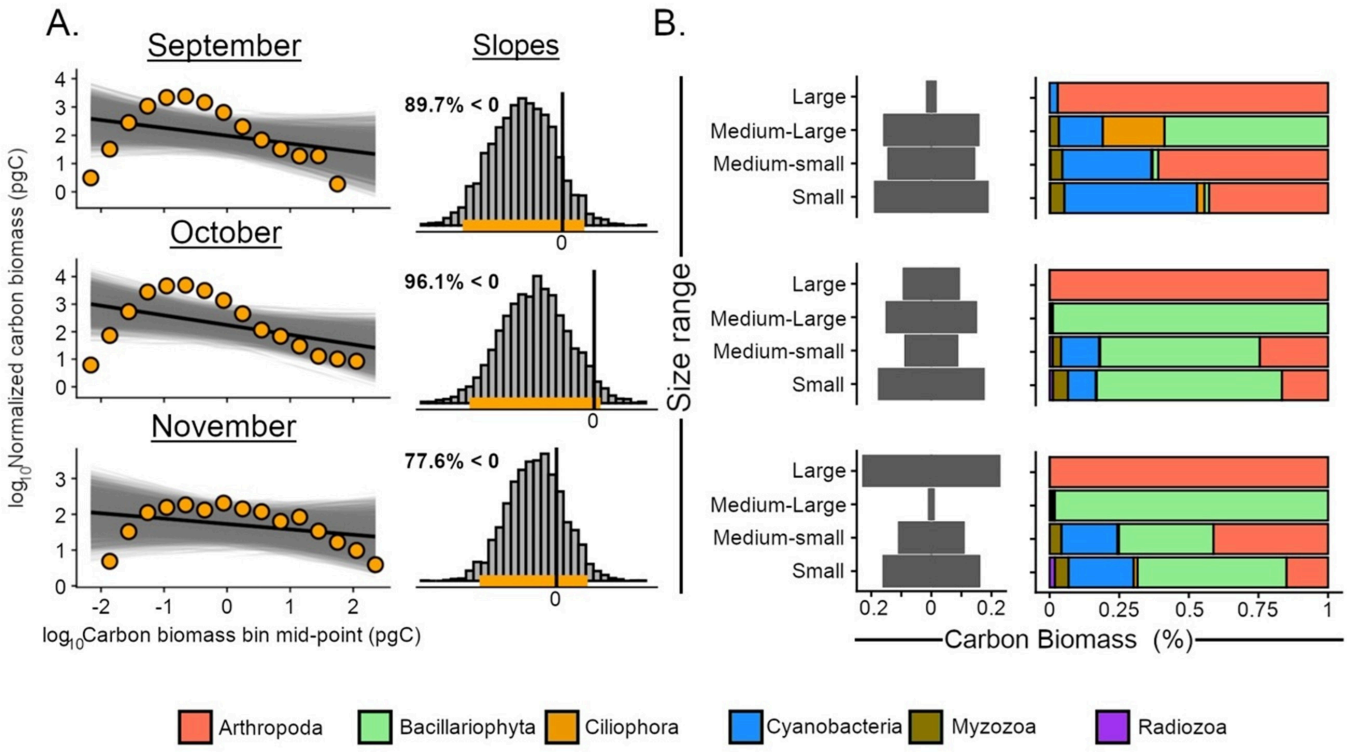

Figure 6

Carbon biomass distribution among body size. (A) Normalized Biomass Size Spectrum (NBSS). Points represent the cumulative representation of size bins and their respective normalized biomass. Thin grey lines show the predicted fits from Bayesian linear models, and black thick lines illustrate the mean fit values. Histograms of the Bayesian estimated slopes are also shown, with the horizontal thick orange lines representing the 95% confidence interval. Proportions of negative slopes are indicated. (B) Illustration of biomass distribution per coarse size ranges with their respective Phylum composition.

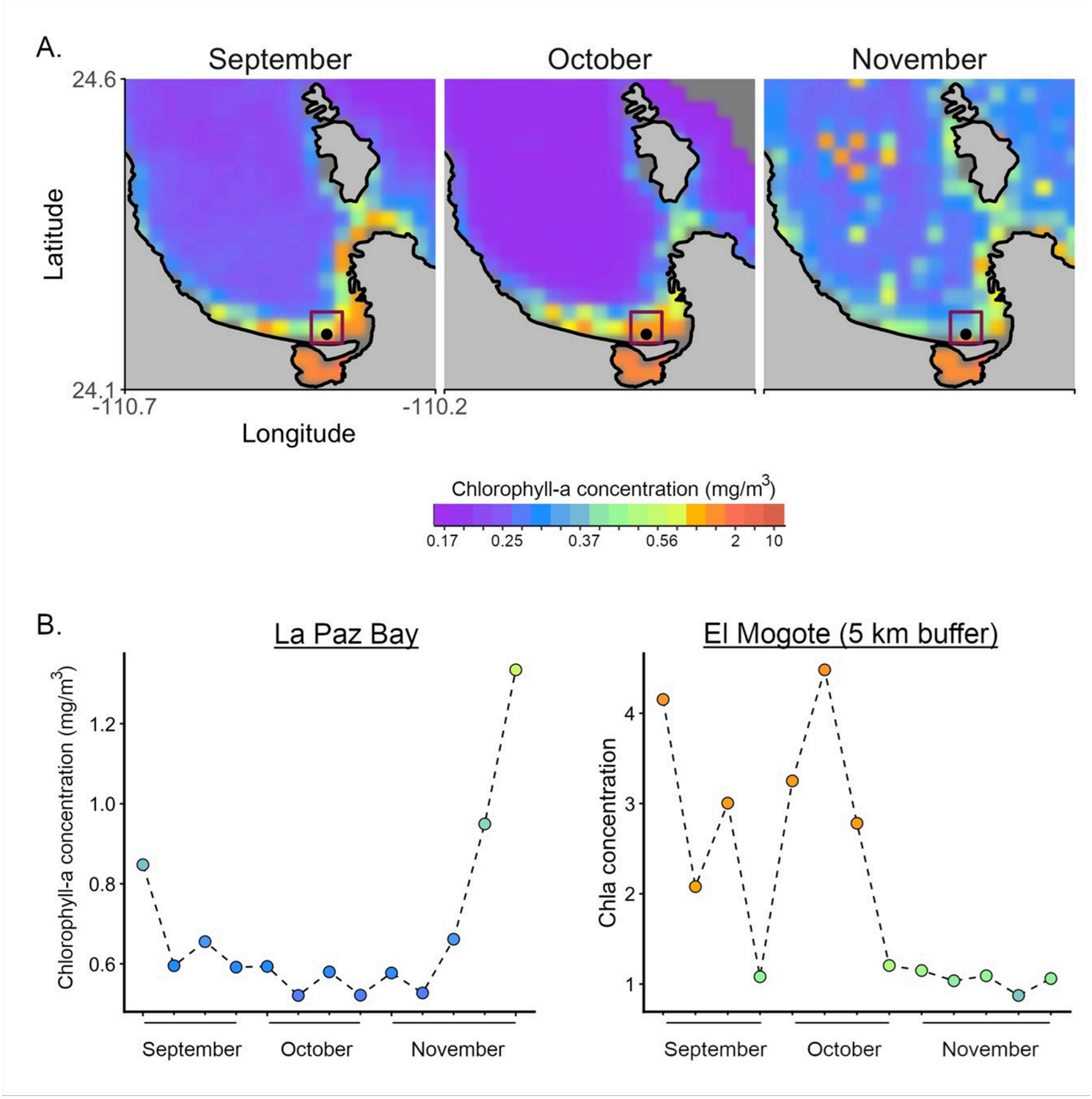

Figure 7

Chlorophyll-*a* (Chl-*a*) concentrations in the Bay of La Paz during the sampling period. (A) Spatial distribution of mean Chl-*a* concentration per month in the Bay of La Paz. (B) Temporal variation of Chl-*a* concentration for each week in the Bay of La Paz and within a 5 km buffer zone surrounding the sampling site. In panel A, the black dot highlights the sampling location and the 5 km buffer excluding land is indicated by a purple square. Chl-*a* concentrations come from: https://coastwatch.pfeg.noaa.gov/data.html.